

Design and Performance of a Biomass-based Polygeneration System for Simultaneous Dme and Power Production

*Original*

Design and Performance of a Biomass-based Polygeneration System for Simultaneous Dme and Power Production / Ciccone, Biagio; Scognamiglio, Stefano; Landi, Gianluca; Ruoppolo, Giovanna. - In: CHEMICAL ENGINEERING TRANSACTIONS. - ISSN 2283-9216. - ELETTRONICO. - 109:(2024), pp. 223-228. [10.3303/CET24109038]

*Availability:*

This version is available at: 11583/2989648 since: 2024-06-18T10:18:52Z

*Publisher:*

AIDIC

*Published*

DOI:10.3303/CET24109038

*Terms of use:*

This article is made available under terms and conditions as specified in the corresponding bibliographic description in the repository

*Publisher copyright*

(Article begins on next page)

# Design and Performance of a Biomass-based Polygeneration System for Simultaneous DME and Power Production

Biagio Ciccone<sup>a,b,\*</sup>, Stefano Scognamiglio<sup>a,b</sup>, Gianluca Landi<sup>b</sup>, Giovanna Ruoppolo<sup>b</sup>

<sup>a</sup>Dipartimento di Scienza Applicata e Tecnologia (DISAT), Politecnico di Torino, C.so Duca degli Abruzzi 24-10129, Torino, Italia

<sup>b</sup>Istituto di Scienze e Tecnologie per l'Energia e la Mobilità Sostenibili, Consiglio Nazionale delle Ricerche, P. le V. Tecchio, 80-80125 Napoli, Italia

[biagio.ciccone@stems.cnr.it](mailto:biagio.ciccone@stems.cnr.it)

The present work deals with the preliminary design, the simulation, and the assessment of the thermodynamic performance of a polygeneration system for the simultaneous production of a range of valuable chemical products (namely, di-methyl-ether (DME), methanol (MeOH), H<sub>2</sub>-CH<sub>4</sub> mixtures with an H<sub>2</sub> content up to 30 % – usually referred to as “hythane”) alongside the generation of multiple energy carriers such as heating and power. The system included a biomass gasification step, a steam cycle for power generation, an oxyfuel combustor, a syngas-to-DME section and a methanation section. A sensitivity study on the gasification section showed that low pressure oxygen/steam gasification at 950°C yields a good quality syngas with an H<sub>2</sub>/(CO+CO<sub>2</sub>) ratio of 0.97. A simple graphical method for fixed-bed reactor dimensioning is also presented.

## 1. Introduction

Due to the substantial increase in global emissions and harsh environmental consequences caused by the escalated exploitation of fossil fuels, the research has been focusing on sustainable solutions to match industrial growth and protection of the environment. In this context, polygeneration systems (PGS) hold the potential to simultaneously produce energy carriers and valuable chemicals from renewable biomass sources (Calise et al., 2018). Biomass-based PGS can thus contribute to enhance energy security while fostering sustainability. The existing body of the literature is rich in papers delved into the subject of polygeneration, mostly focusing on the integration of methanol synthesis, Fischer-Tropsch processes and synthetic natural gas, using coal or biomass as starting material. The present work sets the base of a steady-state Aspen Plus model of a biomass-based PGS focused on the simultaneous production of DME, methanol and a combustible H<sub>2</sub>-CH<sub>4</sub> mixture, alongside with heat and power. Particular relevance was given to the sensitivity study on the gasification step because it affects all the processes downstream. A graphical method for the dimensioning of fixed-bed reactors based on theoretical and engineering constraints is also presented in this work.

## 2. Materials and methods

The Aspen Plus simulation flowsheet for the polygeneration system addressed in this study is shown in Figure 1. The gasification process is modelled as a combination of a decomposition reactor (RYield) responsible for converting the feedstock (rice straw) into its respective components by defining the mass-base yield distribution, and an equilibrium reactor (RGibbs) where the syngas is generated. This approach is common in the literature (Parvez et al., 2016). Rice straw, entering the system at a rate of 1000 kg h<sup>-1</sup>, is fed into the gasification process alongside steam and oxygen produced from a renewable energy-driven electrolysis system. This autothermal process yields high-temperature syngas, which subsequently undergoes ash removal (Sep) before being employed as an energy source in a Hirn cycle for power generation. The hot syngas is then directed to a cleaning section designed to eliminate sulphur compounds, nitrogen compounds, and other impurities, such as chlorine. Tar formation is not considered in the simulation. This cleaning section is represented as a simple separator in the Aspen Plus model. A fraction of the purified syngas is utilized as fuel in the oxy-combustor, while the rest is

divided and channelled into the DME synthesis and methanation stages. The oxyfuel combustor is simulated using the RStoic module in Aspen Plus with complete conversion of the reactants and operates at 1 bar. Pure oxygen, produced via electrolysis, is employed for combustion. The resulting flue gas is cooled by a heat-recovery unit, and the condensed water is separated, leaving behind a  $\text{CO}_2$ -rich stream (95 % vol.). Part of this  $\text{CO}_2$ -rich stream is recycled to the reactor inlet to keep oxygen concentration low for safety reasons. The methanation unit includes a recycle adiabatic fixed-bed reactor followed by a condenser for water removal and a second adiabatic reactor to enhance the conversion of  $\text{CO}$  and  $\text{CO}_2$ . The recycle ratio in the first reactor is set as the control variable to limit the maximum temperature to 550 °C. Higher temperatures could lead to the deactivation of the  $\text{Ni-Al}_2\text{O}_3$  methanation catalyst (Rönsch et al., 2016). Methanation catalyst data used in the simulation were retrieved from the literature and are reported in Table 1 (Matthischke et al., 2018). The goal of this section is the production of easy-to-stock combustible  $\text{H}_2$ - $\text{CH}_4$  mixtures.

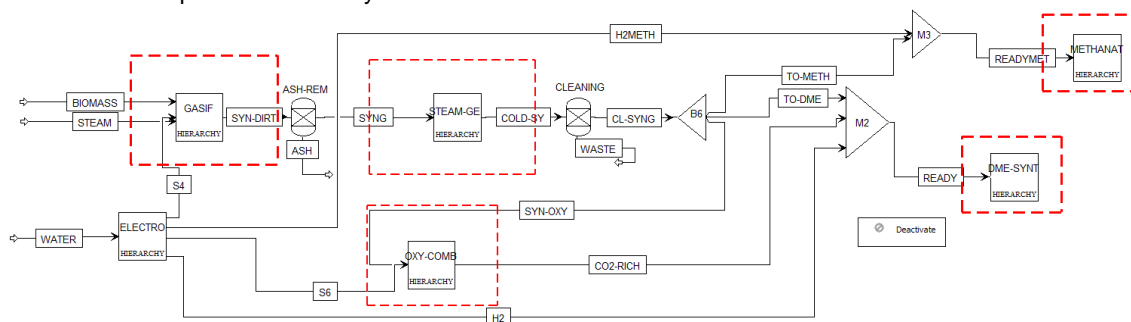


Figure 1: Simulation flowsheet for the biomass-based polygeneration system.

Table 1: Modelling assumptions and operating parameters of the biomass-based polygeneration system.

Key component	Aspen Unit	Operating conditions	Other parameters
Gasifier	RYield, RGibbs	950°C, 1 bar	
Electrolyser	RStoic	40°C, 2.5 bar	Fractional conversion of $\text{H}_2\text{O}$ is 1.
Oxyfuel combustor	RStoic	Adiabatic, 1 bar	
Oxyfuel condenser	Flash2	20°C, 1 bar	
Steam generator (boiler)	HeatX (design)	$\Delta P \approx 0$	Specified cold stream outlet temperature: 410 °C.
Steam turbine	Compr	Discharge pressure 0.05 bar.	Isentropic efficiency: 0.85.
Steam condenser	Flash2	0.05 bar	Vapor fraction: 0
Water pump	Pump	Discharge pressure: 20 bar;	Pump efficiency: 0.85.
Syngas cleaning	Sep		Split fraction of waste (C, S, $\text{Cl}_2$ ) is 1.
Methanation reactor (PFR1)	RPlug	Adiabatic	Length: 0.35 m; Diameter: 0.57 m. Bed void fraction: 0.39, catalyst particle density: 1475 $\text{kg}/\text{m}^3$ , particle diameter: 3 mm. Mole-based recycle ratio: 5.6. Catalyst mass: 131.7 kg
Methanation reactor (PFR2)	RPlug	Adiabatic	Length: 0.37 m; Diameter: 0.18 m. Bed void fraction: 0.39, catalyst particle density 1475 $\text{kg}/\text{m}^3$ , particle diameter: 3 mm. Catalyst mass: 13.9 kg.
Water condenser (methanation)	Flash2	90°C, 5 bar	
Syngas compressor (DME)	Compr	Discharge pressure: 50 bar.	Isentropic efficiency: 0.85.
DME synthesis reactor	RPlug	Isothermal (250°C) 50 bar	Catalyst weight: 651 kg; Diameter: 0.3 m. Bed void fraction 0.4, catalyst particle density 1982.5 $\text{kg}/\text{m}^3$ , particle diameter: 2 mm
DME/MeOH distillation	Sep		Ideal separation.

For the DME synthesis, the direct synthesis method is applied, which involves the use of a bifunctional catalyst. This catalyst simultaneously facilitates the hydrogenation of carbon oxides to methanol and the subsequent methanol dehydration to dimethyl ether (DME) in a single fixed bed catalytic reactor.

This process is thermodynamically and economically more favourable than the two-step process (Wang et al., 2011). The data for the commercial bifunctional Cu-ZnO/Al<sub>2</sub>O<sub>3</sub> catalyst was retrieved from Mevawala et al. (2017) and it is available in Table 1, which also summarizes the main parameters for the different sections of the polygeneration system. Particular attention was devoted to the sizing of the fixed-bed reactors (DME synthesis and methanation), as reported in the Appendix.

The proximate and ultimate analysis for the rice straw is reported in Table 2. The stream class was set as MIXCINC because both conventional and non-conventional solids are present, but no particle size distribution is considered. The Peng-Robinson equation of state with Boston – Mathias modifications was employed as thermodynamic method of calculation because it is suitable for nonpolar or mildly polar gas mixtures (e.g., syngas) (Aspen Tech, 2010). The feed stream ‘Biomass’ is defined as non-conventional solid.

Table 2: Proximate and ultimate analysis of rice straw (Parvez et al., 2016)

Proximate analysis	Content [wt% dry basis]	Ultimate analysis	Content [wt% dry basis]
Moisture content	8.9	C	45.1
Volatile matter	76.6	H	6.2
Fixed carbon	10.4	O (by difference)	32
Ash	13.0	N	3.1
		S	0.6

### 3. Results and discussion

#### 3.1 Sensitivity analysis (gasification)

A sensitivity analysis was conducted to investigate the impact of operating parameters on the quality of the produced syngas during the gasification step. Figure 2 illustrates the influence of the gasification temperature, the steam/ biomass ratio (S/B) and the equivalence ratio (ER) on the H<sub>2</sub>/CO/CO<sub>2</sub> ratios of the resulting syngas.

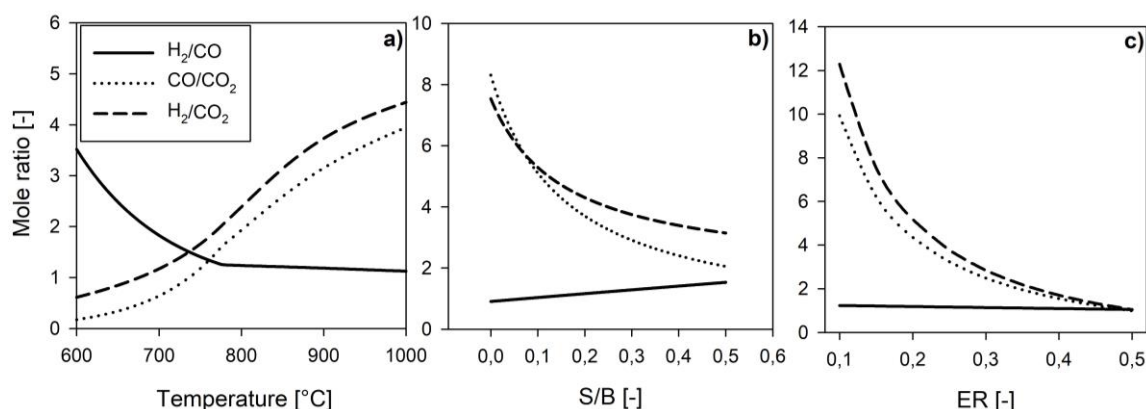


Figure 2: Effect of the gasification temperature (a), the steam/biomass ratio (b) and the equivalence ratio (c) on the syngas quality.

Temperature plays a crucial role in determining the molar composition of the syngas due to its influence on the thermodynamic equilibrium of the system (Figure 2a). Higher temperatures favor endothermic reactions such as the steam reforming of methane and methane cracking, resulting in a syngas rich in H<sub>2</sub> and CO. Conversely, methane content decreases with temperature, as methanation reactions ( $\text{CO} + 3\text{H}_2 \rightarrow \text{CH}_4 + \text{H}_2\text{O}$  and  $\text{CO}_2 + 4\text{H}_2 \rightarrow \text{CH}_4 + 2\text{H}_2\text{O}$ ) are highly exothermic. As reported in the literature, higher gasification temperatures lead to lower H<sub>2</sub>/CO ratio (Gröbl et al., 2012).

The steam/biomass ratio (S/B), here defined as the ratio between added steam and the as-received biomass mass flow, is a pivotal parameter in steam gasification. Higher S/B enriches the system with hydrogen molecules derived from steam, promoting water-gas shift ( $\text{CO} + \text{H}_2\text{O} \rightarrow \text{CO}_2 + \text{H}_2$ ) and steam reforming reactions ( $\text{CH}_4 + \text{H}_2\text{O} \rightarrow \text{CO} + 3\text{H}_2$ ), leading to increased hydrogen production. Therefore, the H<sub>2</sub>/CO ratio increases with S/B, as illustrated in Figure 2b.

The equivalence ratio (ER), defined as the ratio between the oxygen content in the oxidant supply and the stoichiometric amount for complete combustion, deeply influences the syngas quality as it tunes the relative

importance of partial oxidation over the steam reforming reactions in the O<sub>2</sub>/steam gasifier. The higher the ER, the higher the contribution of partial oxidation in the reaction network, which leads to higher CO<sub>2</sub> production and less H<sub>2</sub> in the produced syngas, as shown in Figure 2c.

To achieve a syngas composition suitable for subsequent DME and SNG synthesis, namely, high H<sub>2</sub> content and low CO<sub>2</sub> content, low pressure and high temperature conditions were selected. The steam/biomass ratio (S/B) and the equivalence ratio (ER) were set to 0.2. The optimal syngas composition for the direct DME synthesis (H<sub>2</sub>/CO=4 and CO/CO<sub>2</sub>≈1) and for the methanation step (H<sub>2</sub>/CO/CO<sub>2</sub>=7/1/1 and low CO<sub>2</sub>/CO) are obtained by mixing the syngas with pure hydrogen and CO<sub>2</sub> (95%), as shown in Figure 1.

### 3.2 Global material balance.

The results of the material balance for the polygeneration system of Figure 1 are reported in Figure 3. As highlighted by the Sankey diagram, the preliminary polygeneration system addressed in this study produces - per kg of dry biomass in the feed - 0.11 kg of DME, 0.026 kg of MeOH, 0.28 kg of hythane (34.3% H<sub>2</sub> and 54.7% CH<sub>4</sub> on a dry basis). Moreover, 95% pure CO<sub>2</sub>, water and a CO<sub>2</sub>/H<sub>2</sub> stream are also side products of the system, which can be used for different applications. In the preliminary phase of the design, major importance was given to the optimization of the single units within the system of Figure 1. A future work will delve into the overall optimization of the system both from a thermodynamic perspective, by evaluating the energy and exergy efficiencies, and from a techno-economic perspective, by studying strategies to reduce wastes and costs. Despite this process is still to be optimized, these preliminary results clearly show that a significant production of fuels can be obtained; moreover, a high-purity CO<sub>2</sub> stream and a CO<sub>2</sub>/H<sub>2</sub> stream (68.2% H<sub>2</sub> 28.4% CO<sub>2</sub>) are produced, that can be further processed and/or stored, thus allowing a neutral and/or negative carbon balance.

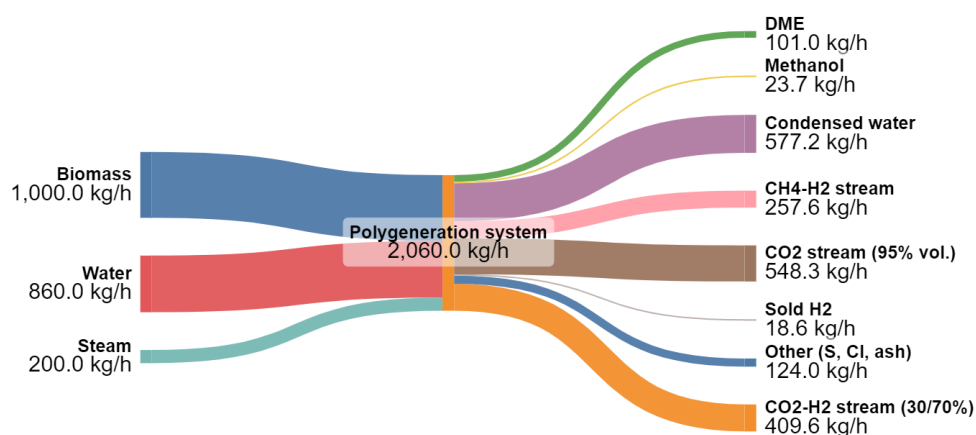


Figure 3: Sankey diagram for the biomass-based polygeneration system.

## 4. Conclusions

In this work a preliminary steady-state model of a polygeneration system based on the gasification of rice straw is illustrated. An equilibrium approach is used to model the gasification step, and the effect of the most significant operating conditions (namely, temperature, S/B and ER) has been investigated through a sensitivity study. Results show that low pressure oxygen/steam gasification (S/B=0.2, ER=0.2) at 950°C yields a syngas predominantly composed of H<sub>2</sub> (41.7%), CO (35.0%), H<sub>2</sub>O (13.8%) and CO<sub>2</sub> (8.0%). Although the overall system is not optimized, it is the starting point for future techno-economic and thermodynamic analysis. A simple graphic design method for fixed-bed reactors is also presented in this work.

## Acknowledgments

Project funded by the European Union – NextGenerationEU under the National Recovery and Resilience Plan (NRRP), Mission 4 “Education and Research” - Component 2 “From research to business” - Investment 3.1 “Fund for the realization of an integrated system of research and innovation infrastructures” - Call n. 3264 of 28/12/2021 of Italian Ministry of University and Research | Award Decree n. 128 (21/06/2022) - Project code: IR0000027 - CUP: B33C22000710006 - Project title: iENTRANCE@ENL: Infrastructure for Energy TRAnSition aNd Circular Economy @ EuroNanoLab

## Nomenclature

$d_p$ - particle diameter, mm	$U_0$ - superficial velocity, m/s
$D_t$ - reactor diameter, m	$V$ - reactor volume, m <sup>3</sup>
$K_i$ - regression analysis constant, -	$y_P$ - product mole fraction, -
$L$ - reactor length, m	$\Delta P/L$ - pressure drop, bar/m
$L_{eq}$ - minimum reactor length to reach equilibrium, m	$\varepsilon$ - bed void fraction, -
LHV- lower heating value, MJ/Nm <sup>3</sup>	$\mu$ - gas mixture viscosity, Pa s
$Q$ - volumetric flow rate, m <sup>3</sup> /s	$\rho$ - gas mixture density, kg/m <sup>3</sup>
$Q_m$ - mass flow rate, kg/s	$\tau$ - reactor space time, s
$Re_p$ - particle Reynolds number, -	$\phi$ - sphericity factor, -

## References

- Aspen tech, 2010, Aspen physical property system: physical property methods, Version 7.2. Burlington: USA.
- Calise F., di Vastogirardi G., d'Accadia G.D.N., Vicidomini M., 2018, Simulation of polygeneration systems, *Energy*, 163, 290-337.
- Gröbl T., Walter H., Haider M., 2012, Biomass steam gasification for production of SNG—Process design and sensitivity analysis, *Applied Energy*, 97, 451-461.
- Matthischke S., Roensch S., Güttel R., 2018, Start-up time and load range for the methanation of carbon dioxide in a fixed-bed recycle reactor, *Industrial & Engineering Chemistry Research*, 57.18, 6391-6400.
- Mevawala C., Jiang Y., Bhattacharyya D., 2017, Plant-wide modeling and analysis of the shale gas to dimethyl ether (DME) process via direct and indirect synthesis routes, *Applied Energy*, 204, 163-180.
- Parvez A. M., Mujtaba I. M., Hall P., Lester E. H., Wu, T., 2016a, Synthesis of Bio-Dimethyl Ether Based on Carbon Dioxide-Enhanced Gasification of Biomass: Process Simulation Using Aspen Plus, *Energy Technology*, 4.4, 526-535.
- Rönsch S., Schneider J., Matthischke S., Schlüter M., Götz M., Lefebvre J., Prabhakaran P., Bajohr S., 2016, Review on methanation—From fundamentals to current projects, *Fuel*, 166, 276-296.
- Wang T., Li Y., Ma L., Wu C., 2011, Biomass to dimethyl ether by gasification/synthesis technology—an alternative biofuel production route, *Frontiers in Energy*, 5, 330-339.
- Woods, D.R., 2007, Rules of thumb in engineering practice. John Wiley & Sons, USA.

## Appendix

This appendix illustrates the procedure for the choice of the appropriate values of the diameter and the length of the fixed bed reactors present in the system (both in the methanation section and the DME section). The sizing method considers some relevant guidelines for good industrial practice in reactor dimensioning (e.g., Woods, 2007) and chemical engineering considerations, as reported in Table 3:

Table 3: Guidelines for good industrial practice of fixed bed catalytic reactors (adapted from: Woods, 2007).

Condition n°	Factor	Suggested guidelines
1	Catalyst pellet diameter, $d_p$	Should be 1-5 mm
2	The space-time of the reactor, $\tau = \frac{V}{Q}$	Should be kept < 1 s
3	$D_t/d_p$	Should be kept > 10
4	Pressure drops, $-\frac{\Delta P}{L}$	Should be kept < 10%
5	$L/d_p$	Should be kept > 100
6	Effective reactor length, L	Should enable to reach equilibrium (i.e., $L=1.1 L_{eq}$ )
7	Particle Reynolds number, $Re_p$	Should be kept > 100 to ensure turbulent regime

All the physical properties are evaluated at the mean temperature between the reactor inlet and outlet. The procedure involves the graphical representation of a region of possible designs in the  $L$ - $D_t$  plane, where all the

conditions in Table 3 are met. Conditions from Table 3 are hereafter rearranged for suitable graphical representation. While conditions 1-5 and 7 are easily rearranged, condition 6 is approached with an iterative process. The acceptable range for the reactor diameter is firstly identified by combining the other conditions. Subsequently, utilizing the Aspen software, the product mole fraction profile along the reactor coordinate is calculated for different reactor diameters, and for each profile the derivative of the product mole fraction with respect to the reactor axial coordinate ( $dy_P/dz$ ) is evaluated. For each diameter, the length ( $L_{eq}$ ) at which  $dy_P/dz$  falls below a specific equilibrium tolerance (e.g., 1% in this study) is determined and a regression analysis is performed to establish a power relationship between reactor diameter and the equilibrium length as reported in Table 4, condition n°6. Once all the conditions have their analytical form in the  $L$ - $D_t$  variables, it is possible to draw the dimensioning plot, from which it is easy to identify the region of the acceptable ( $D_t$ ,  $L$ ) couples for the reactor. For clarity, Table 4 reports the analytical functions derived from the industrial guidelines and the corresponding constants.

Table 4: Functional form of the conditions of Table 3 and corresponding parameters.

Condition n°	Function	Parameters
2	$f(D_t, L) = D_t^2 L - \alpha < 0$	$\alpha = \frac{4Q}{\pi}$
3	$g(D_t, L) = D_t - \beta < 0$	$\beta = 10d_p$
4	$h(D_t, L) = L \left( \frac{\gamma}{D_t^2} + \frac{\delta}{D_t^4} \right) - 0.1P < 0$	$\gamma = \frac{150(1-\epsilon)^2}{\epsilon^3 \phi^2 \pi d_p^2} 4\mu Q$ $\delta = \frac{1.75(1-\epsilon)}{\epsilon^3 \phi d_p} \rho \frac{16Q^2}{\pi^2}$
5	$j(D_t, L) = L - \zeta > 0$	$\zeta = 100d_p$
6	$m(D_t, L) = L - K_1 D_t^{K_2} \geq 0$	$K_1$ and $K_2$ from regression analysis
7	$n(D_t, L) = \frac{\lambda}{D_t^2} - 100 > 0$	$\lambda = \frac{\rho d_p 4Q_m}{\pi(1-\epsilon)\mu}$

As an example, Figure 4 reports the  $D_t$ - $L$  plot for the methanation recycle reactor (PFR1) with a suitable choice for the reactor diameter and length:

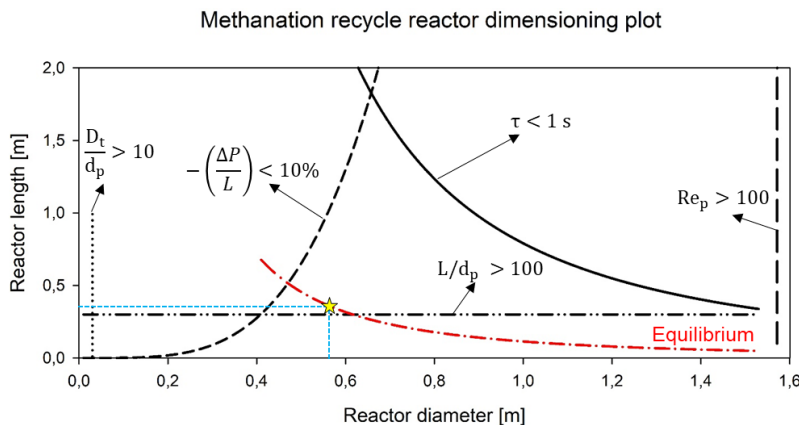


Figure 4: Dimensioning plot for the recycle methanation reactor.